Processing of α4 integrin by the proprotein convertases: histidine at position P6 regulates cleavage

Eric BERGERON*, Ajoy BASAK†, Etienne DECROLY*[1] and Nabil G. SEIDAH*[2]

*Laboratory of Biochemical Neuroendocrinology, Clinical Research Institute of Montreal, 110 Pine Avenue West, Montreal, QC, Canada, H2W 1R7, and †Laboratory of Molecular Medicine and Disease of Ageing Center, Loeb Health Research Institute, Ottawa Civic Hospital, 725 Parkdale Avenue, Ottawa, ON, Canada, K1Y 4K9

The proprotein convertases (PCs) participate in the limited proteolysis of integrin α4 subunit at the $\underline{H}^{592}VIS\underline{KR}^{597}\downarrow ST$ site (where underlined residues indicate positively charged amino acids important for PC-mediated cleavage and $\downarrow$ indicates the cleavage site), since this cleavage is inhibited by the serpin α1-PDX (α1-antitrypsin Portland). Co-expression of α4 with each convertase in LoVo (furin-deficient human colon carcinoma) cells revealed that furin and proprotein convertase 5A (PC5A) are the best pro-α4 convertases. In agreement, processing of endogenous pro-α4 in human lymphoblastoid CEM-T4 cells was enhanced greatly in stable transfectants overexpressing either enzyme. In many leucocyte cell lines, the expression of furin closely correlated with the endogenous processing efficacy, suggesting that furin is a candidate pro-α4 convertase. Mutational analysis showed that replacement of P1 Arg^{597} with alanine (R597A) abrogated cleavage, whereas the P6 mutant H592R is even better processed by the endogenous convertases of Chinese-hamster ovary CHO-K1 cells. *In vitro* kinetic studies using synthetic peptides confirmed the importance of a positively charged residue at P6 and showed that wild-type α4 processing is performed best by furin and PC5A at acidic and neutral pHs, respectively. Biosynthetic analysis of pro-α4 and its H592R and H592K mutants in the presence or absence of the weak base, NH_4Cl, revealed that the P6 histidine residue renders its processing by furin sensitive to cellular pH. This suggests that pro-α4 cleavage occurs preferentially in acidic compartments. In conclusion, although the accepted furin processing motif is Arg-Xaa-(Lys/Arg)-Arg$\downarrow$, our data further extend it to include a regulatory histidine residue at P6 in precursors that lack a basic residue at P4.

Key words: furin, integrin, PC5A, α1-antitrypsin Portland (α1-PDX), pH, precursor processing.

INTRODUCTION

Integrins form a family of cell-surface heterodimeric $\alpha\beta$ adhesion receptors that regulate cell–cell and cell–extracellular matrix (ECM) protein interactions. They have a critical role in various homoeostatic processes, including embryogenesis, tissue remodelling, thrombosis and leucocyte migration, and are involved in diseases such as cancer and inflammatory pathologies [1]. At the present time, 18 α and 8 β subunits are known and can form 24 distinct non-covalent $\alpha\beta$ heterodimers [2]. Of these, two α4-containing receptors have been described: $\alpha4\beta1$ and $\alpha4\beta7$. Expression of $\alpha4\beta1$ is restricted to leucocytes and some adherent cells [3]. Nevertheless, its expression is critical for mouse cardiac and placental development [4]. The other dimer, $\alpha4\beta7$, is only present in a specialized subset of lymphocytes that migrate to the gut mucosa [5]. *In vivo*, $\alpha4\beta1$ and $\alpha4\beta7$ bind to the vascular cell adhesion molecule-1 (VCAM-1) [6] and the mucosal addressin cell adhesion molecule-1 ('MadCAM-1') [5] respectively. In addition, they both bind to the connective segment-1 of the alternatively spliced V region of fibronectin [7].

Nine of the 18 α subunits (α3, α4, α5, α6, α7, α8, αv, αE and αIIb) undergo post-translational endoproteolytic cleavage at a site comprising pairs of basic amino acids (Figure 1). This site is usually close to the C-terminal transmembrane domain, except for αE and α4, where it is at the beginning and in the middle of their ectodomain respectively. Unlike the other cleavable α integrins, pro-α4 (150 kDa) endoproteolysis generates N-terminal (80 kDa) and C-terminal (70 kDa) products that are held together non-covalently (Figure 1) [8–10]. To our knowledge, only processed forms of cleavable α subunits are present at the cell surface, except for α4, whose processing seems to be regulated. For example, quiescent T-lymphocytes express α4 mostly as an unprocessed chain at their cell surface, whereas, upon their *ex vivo* activation with phytohaemagglutinin and interleukin-2, only fully processed α4 is detected at the cell surface [8,10].

Recently, the crystal structure elucidation of the $\alpha v\beta3$ extracellular portion allowed the visualization of its overall three-dimensional structure as an ovoid 'head' with two highly flexible 'tails', which would extend to the plasma membrane in the native integrin [11]. The head is formed by the seven-bladed β-propeller of αv and the A-domain of β3, and is directly responsible for ligand binding [11], whereas the tails are required for outside-in and/or inside-out signal transduction [12]. According to this crystal structure, the αv cleavage site (Arg^{890}) would be close to the membrane [11]. In contrast, based on the $\alpha4/\alpha v$ alignment (results not shown), the α4 processing site would be in a loop in the upper part of the tail, at the interface with the head, suggesting that α4 cleavage may affect head movement and/or flexibility.

Abbreviations used: Abz, 2-aminobenzoic acid; AMC, 7-amino-4-methylcoumarin; BTMD, before transmembrane domain; DMEM, Dulbecco's modified Eagle's medium; ECM, extracellular matrix; ER, endoplasmic reticulum; EGFP, enhanced green fluorescence protein; endoH, endoglycosidase-H; FBS, foetal bovine serum; HRP, horseradish peroxidase; mAb, monoclonal antibody; MCA, 4-methylcoumarin-7-amide; MALDI–TOF-MS: matrix-assisted laser-desorption ionization–time-of-flight MS; PACE, paired basic amino acid cleaving enzyme; PC, proprotein convertase; α1-PDX, α1-antitrypsin Portland; QFP, quenched fluorogenic peptide; RP-HPLC, reverse phase HPLC; RT, reverse transcriptase; TGN, *trans*-Golgi network; Tyx-A, 3-nitro-Tyr-Ala; VCAM-1, vascular cell adhesion molecule-1; VV, vaccinia virus; WT, wild-type.

[1] Present address: INSERM U372, Pathogénie des Infections à Lentivirus, Parc Scientifique et Technologique de Luminy, 163 Avenue de Luminy, 13276 Marseille, Cedex 9, France.

[2] To whom correspondence should be addressed (e-mail seidahn@ircm.qc.ca).

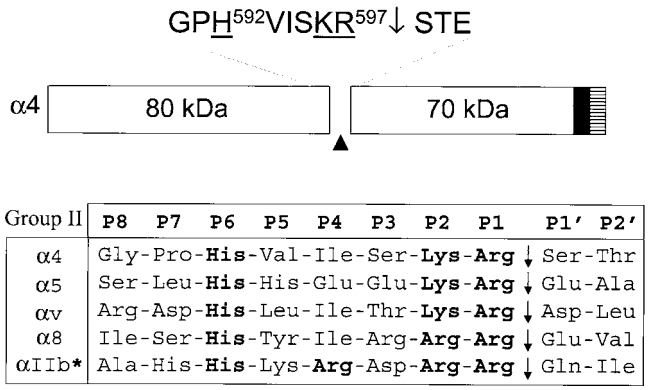

Group II	P8	P7	P6	P5	P4	P3	P2	P1	P1′	P2′
α4	Gly	Pro	**His**	Val	Ile	Ser	**Lys**	**Arg** ↓	Ser	Thr
α5	Ser	Leu	**His**	His	Glu	Glu	**Lys**	**Arg** ↓	Glu	Ala
αv	Arg	Asp	**His**	Leu	Ile	Thr	**Lys**	**Arg** ↓	Asp	Leu
α8	Ile	Ser	**His**	Tyr	Ile	Arg	**Arg**	**Arg** ↓	Glu	Val
αIIb*	Ala	His	**His**	Lys	**Arg**	Asp	**Arg**	**Arg** ↓	Gln	Ile

Figure 1 Schematic representation of α4 and alignment of group II α integrins

The processing sites (arrows), transmembrane domains (black box) and cytosolic tails (hatched box) are emphasized. The basic and histidine residues present in the α4 cleavage site are underlined. The sequences surrounding human α integrin cleavage sites containing a P6 histidine residue (group II) are aligned. Note that αIIb(*) is phylogenetically closer to group II members (see text).

Alignment of the cleavable α integrin sequences (using PileUp and GrowTree GCG programs; http://helix.nih.gov/docs/gcg/) suggested the existence of two phylogenetic groups that present distinct consensus cleavage sites: Arg-Xaa-(Lys/Arg)-Arg↓ for group I members (α3, α6, α7 and αE) and His-Xaa-Xaa-Xaa-(Lys/Arg)-Arg↓ for group II members (α4, α5, αv, α8 and αIIb) (Figure 1). Thus the presence of a P4 arginine or a P6 histidine residue is a distinguishing feature of each group, except for αIIb (group II), which exhibits both of them. Furthermore, group I members were shown to bind ECM proteins that do not exhibit RGD (Arg-Gly-Asp) or LDV (Leu-Asp-Val) motifs, e.g. laminin [2]. Although it is presently unclear for α4, other group II α integrins can bind ligands in an RGD-dependent fashion [2].

A family of proprotein convertases (PCs), which are Ca^{2+}-dependent serine proteinases related to the yeast subtilisin-like kexin, exhibit a cleavage specificity for the consensus sequence (**Arg/Lys**)-$(Xaa)_n$-(**Lys/Arg**)↓, where n = 0, 2, 4 or 6, compatible with that of integrin cleavage sites and emboldening indicates positively charged amino acids. So far, seven basic amino-acid-specific PCs are known: furin [or paired basic amino acid cleaving enzyme (PACE)], PC1 (PC3), PC2, PC4, PACE4, PC5 (PC6) and PC7 (LPC, PC8) (reviewed in [13,14]). They are responsible for the limited intracellular proteolysis of a large number of precursors. With the exception of PC1 and PC2, the other PCs are present in the constitutive secretory pathway and may thus be candidate convertases for integrin processing. However, unlike other PCs, PC1 and PC2 are found mostly in the regulated secretory pathway of neural and endocrine cells. Indeed, *ex vivo* studies revealed that furin [15,16] and PC5A [15] process αv, α5 and α6, and possibly α3 integrins [16]. Biosynthetic analysis of α4 and other α subunits have established that the cleavage occurs in post-endoplasmic reticulum (ER) compartments [9,16,17] and that α4 processing is sensitive to organelle pH [9]. Similar to pro-α4 cleavage, furin activation also occurs in post-ER compartments and requires mildly acidic pH [18]. These results suggested that pro-α4 processing enzymes are active in acidic compartments and/or its cleavage requires low pH.

The physiological consequences of pro-α subunit processing are still obscure, as unprocessed α4β1 can reach the cell surface to bind to VCAM-1 and fibronectin [8], and, similarly, pro-α6β1 can bind to laminin-1 [19]. On the other hand, uncleaved α6β1 does not exhibit inside-out signalling following PMA activation. This suggests that cleavage of pro-α6 is required to generate a proper conformation that enables the affinity modulation of the α6β1 receptor by PMA [19]. It has also been shown that the inhibition of pro-α processing in HT-29 cells stably expressing the PC inhibitor α1-PDX (α1-antitrypsin Portland) [20–22] decreased adhesion to vitronectin *in vitro*, but not to other ECM proteins such as laminin-1 and collagen type I [23]. This diminished adhesion to vitronectin was explained by the inability of unprocessed pro-αv to stimulate phosphorylation of the focal adhesion kinase and the downstream mitogen-activated protein kinases. Since α1-PDX was used in these earlier experiments, it was not possible to rule out a probable pleiotropic effect of this serpin, as PCs are responsible for the activation of a variety of cellular protein precursors involved in cell signalling [13,24] that may modulate integrin adhesion [25].

In the present study, we first determined that furin and PC5A are the main cellular convertases responsible for the processing of α4β1 integrin. This observation was confirmed further by the analysis of endogenous pro-α4 processing in human lymphoblastoid CEM-T4 cells stably expressing either PC. *In vitro*, both furin and PC5A effectively processed synthetic peptides encompassing the cleavage site. Kinetic analysis revealed that, at acidic pH, furin is best suited to cleave at the $H^{592}VISKR^{597}$ ↓ ST site (where underlined residues indicate positively charged amino acids important for PC-mediated cleavage and ↓ indicates the cleavage site), whereas PC5A prefers neutral pH conditions. In addition, in leucocyte-derived cell lines, furin expression correlates with the extent of pro-α4 processing. Site-directed mutagenesis demonstrated the critical importance of P1 arginine and P6 histidine residues for pro-α4 processing and established that the P6 histidine residue restricts the site of cleavage of pro-α4 by furin to acidic compartments. Finally, we also found that in Chinese-hamster ovary CHO-K1 cells, an uncleavable P1 $Arg^{597} \rightarrow$ Ala (R597A) α4 mutant does not affect the *in vitro* adhesion of α4β1 to VCAM-1.

EXPERIMENTAL

Recombinant plasmid construction and site-directed mutagenesis

Human α4 cDNA (ATCC, Manassas, VA, U.S.A.) was transferred from pBluescriptKS$^-$ (*Sal*I/*Xba*I) to the vaccinia virus (VV) vector pMJ601 (*Sal*I/*Nhe*I) [21]. Oligonucleotides were designed to replace, using PCR, either His^{592} with Arg, Lys, Glu, Ala and Leu, or Arg^{597} with Ala. Silent mutations were sometimes introduced to facilitate the screening with restriction endonucleases. Mutated nucleotides are underlined in the following sense primers: H592R, 5′-CCTTGGTCCTCGAGTCATCAG-3′; H592K, 5′-CCACCTTGGTCCTAAAGTCATCAG-3′; H592E, 5′-CCACCTTGGTCCCGAGGTCATCAG-3′; H592A, 5′-CCTTGGTCCTGCTGTGATCAG-3′; H592L, 5′-CCACCTTGGTCCTCTTGTC-3′; R597A, 5′-CCACCTTGGTCCTCATGTCATCAGTAAAGCTAGTACAG-3′. These, and the antisense primer, 5′-ATGCATCATCTCCAGCATTAAA-3′, were used for PCR amplifications from the PMJ601-α4 vector template, and PCR products were cloned in the pCRII-TOPO vector (Invitrogen, Burlington, ON, Canada). *Sty*I and *Nsi*I digestion of the recombinant vectors generated a 264 bp fragment that was then substituted for that of the original pBluescriptKS-α4 vector or PMJ601-α4 in the case of the H592R mutant. Mutant cDNAs were finally transferred into the bicistronic mammalian expression vector pIRES2-EGFP (enhanced green fluorescent protein; Clontech, Palo Alto, CA, U.S.A.) using *Xho*I and *Sac*II sites or *Sal*I and *Sac*II sites for

wild-type (WT) α4 and its H592R mutant. Human furin and mouse PC5A cDNAs [21] were also subcloned into the pIRES2-EGFP vector between *Eco*R1 and *Sal*I sites. The pECE-β1 vector (a gift kindly provided by Dr E. Ruoslahti, Cancer Research Center, The Burnham Institute, La Jolla, CA, U.S.A.) was used as a template for PCR amplification of the human β1 cDNA that was then subcloned into the pIRES2-EGFP vector between the *Xho*I and *Eco*RI sites.

Antibodies and cell culture

Mouse monoclonal antibody (mAb) anti-(α4 integrin) (HP2/1) and Cy5-labelled goat anti-mouse IgG conjugate were purchased from Amersham Biosciences (Baie d'Urfé, QC, Canada). All cell culture media were purchased from Canadian Life Technologies (Burlington, ON, Canada). CCRF-CEM (ATCC number CCL-119), CEM-T4 [21], human T-lymphoblastoid SupT1 [21], Jurkat (ATCC number TIB-152), human promyelocytic leukaemia HL-60 (ATCC number CCL-240) and U937 (ATCC number CRL-2367) cells were grown in RPMI 1640 medium supplemented with 10% (v/v) foetal bovine serum (FBS; Wisent, St.-Bruno, QC, Canada). Furin-deficient human colon carcinoma LoVo-C5 cells were cultured in Dulbecco's modified Eagle's medium (DMEM) containing 10% (v/v) FBS. CHO-FD11/Furin cells and Jurkat stable transfectant of α1-PDX cells were cultured as described in [26,27]. Vector, α4 and R597A stably transfected CHO-K1 cells were grown in Ham's F12 medium supplemented with 10% (v/v) FBS and 400 μg/ml Geneticin® (G418; Canadian Life Technologies). All media were supplemented with 25 μg/ml gentamycin (Wisent) and were cultured at 37 °C in 5% CO_2.

VV infections, transfections and FACS

Approx. 80% confluent LoVo-C5 cells were co-infected with WT, α4 and PCs recombinant VVs [21] using 1 plaque-forming unit (pfu) of each stock, and harvested 16 h later for cell surface biotinylation (see below). WT or recombinant pIRES2-EGFP vectors (7 μg) were transfected in CHO-K1 cells in 60 mm diameter plates using LIPOFECTAMINE™ 2000 reagent (Invitrogen). Cells were either biotinylated 48 h later (see below) or selected with 400 μg/ml Geneticin®. Drug-selected cells were submitted to two rounds of FACS with a MoFlo cell sorter (Cytomation, Fort Collins, CO, U.S.A.) to obtain stable pools of similar human α4 integrin immunoreactivity (HP2/1) using a Cy5-labelled secondary antibody. CEM-T4 cells (2.5×10^7) were electroporated with a single pulse of 320 V and 960 μF in 500 μl of RPMI 1640 medium containing 50 μg of furin or PC5A recombinant pIRES2-EGFP vector linearized with *Ase*I (Gene Pulser apparatus; Bio-Rad, Mississauga, ON, Canada). After 48 h, electroporated cells were seeded in complete RPMI 1640 medium supplemented with 800 μg/ml Geneticin®. After 10 days, 10^5 EGFP-positive cells from each transfection underwent FACS to select pools of similar EGFP mean of fluorescence intensity.

Biotinylation assays, immunoprecipitations

Cells growing in suspension were labelled with biotin as described in [16]. Adherent cells were labelled directly in plates. In brief, 5×10^7 cells were incubated with 0.5 mg/ml sulphosuccinimidyl-6-(biotinamido)hexanoate (Pierce, distributed by Biolynx, Brockville, ON, Canada) for 1 h at 4 °C with agitation in PBS containing 2 mM $MgCl_2$. Cells were then lysed on ice for 30 min in lysis buffer [50 mM Tris/HCl, pH 7.4, 1% (v/v) Nonidet P40, 150 mM NaCl, 0.1% (v/v) SDS] containing a Complete™ Protease Inhibitor Cocktail (Roche Diagnostics GmbH, Mannheim, Germany). Alternatively, cells were lysed in SDS- and EDTA-free buffer to maintain α4β1 association [8]. Clarified cell lysates were incubated with the HP2/1 mAb and were precipitated with Protein G Plus/Protein A–agarose beads (Calbiochem, San Diego, CA, U.S.A.). The immunoprecipitated proteins were finally resolved by SDS/PAGE (6% gel) and transferred on to nitrocellulose membranes (Hybond ECL; Amersham Biosciences). Biotinylated proteins were revealed with streptavidin–horseradish peroxidase (HRP) conjugate and enhanced chemiluminescence (ECL Plus™) (both from Amersham Biosciences). ECL Plus™ chemiluminescence or fluorescence was detected by film exposure or Storm™ imaging (Amersham Biosciences) respectively. Fluorescence was quantified with the ImageQuant™ software (Amersham Biosciences). Taking into account the free N-terminus and the presence of 26 and 56 lysine residues in the 80 kDa fragment or in the 150 kDa precursor respectively, the ratio of processed extracellular α4 was calculated as (80 kDa band intensity/27) to (150 kDa band intensity/57 + 80 kDa band intensity/27). The absence of a bias in the biotinylation process in favour of cleaved or uncleaved α4 was evidenced by Coomassie Blue (Sigma-Aldrich, Oakville, ON, Canada) quantification of the 150 and 80 kDa bands after α4 immunoprecipitation and SDS/PAGE (6% gel) separation. The percentage of cleavage obtained by each method differed by only 2%. For radiolabelled α4, band intensities were detected by Storm™ imaging after exposure to a phosphor screen (Amersham Biosciences) and normalized to the number of cysteine and methionine residues.

Northern blot and reverse transcriptase (RT)-PCR

Northern blot analysis of furin, using a 1.1 kb cRNA probe corresponding to the antisense of nucleotides 762–1839 of human furin, and RT-PCR of PC5, PACE4 and PC7 mRNAs were performed as described in [28,29].

Peptide synthesis and purification

The three 17-amino-acid-long peptides [LGP**X**VISKRSTEEF-PLQ, where **X** is His, Arg or Ala] were synthesized on a solid-phase automated peptide synthesizer (Pioneer model, PE-PerSeptive Biosystems, Framingham, MA, U.S.A.) and purified by reverse phase-HPLC (RP-HPLC) [30]. To obtain an intramolecularly quenched fluorogenic peptide (QFP), a 2-aminobenzoic acid (Abz) donor and a 3-nitro-Tyr-Ala (Tyx-A) acceptor group were attached, respectively, to the N- and C-termini of a peptide encompassing the α4 cleavage site (α4-QFP: Abz-GPHVISKR^{597} ↓ STE-Tyx-A) and its P6 His → Arg mutant (α4-QFP-H592R: Abz-GPRVISKR^{597} ↓ STE-Tyx-A) [26,31].

Enzymic assays, Michaelis–Menten constant determination

Secreted mouse PC5A and human furin-BTMD (before transmembrane domain) were collected from VV-infected African green monkey kidney BSC40 cells for enzymic assays [21]. All peptide digestions were made in 96-well plates, in 100 μl of 50 mM Mes and 50 mM Hepes buffer, containing 2 mM $CaCl_2$, adjusted to pH 6.0 or 7.4. Initial rate determinations were obtained with increasing concentrations of either α4-QFP or α4-QFP-H592R (0.3–25.7 μM) at room temperature (22 °C) with a

quantity of enzyme releasing 0.5 nmol/h of 7-amino-4-methylcoumarin (AMC) from the pERTKR–4-methylcoumarin-7-amide (MCA) substrate [29]. The fluorescent C-terminal products of α4-QFP and α4-QFP-H592R cleavage were quantified on a Spectramax Gemini EM spectrofluorimeter (Molecular Devices, Sunnyvale, CA, U.S.A.) using 320 and 420 nm as excitation and emission wavelengths respectively [31]. The initial rate (V_0) was determined using least-squares regression analysis of the spectrometer data recorded from 0 to 120 s after enzyme addition [31]. Kinetic parameters K_m (app) and V_{max} (app) were determined with Grafit4 software (Erithacus Software, Horley, Surrey, U.K.). The data obtained were fitted to the hyperbolic Michaelis–Menten rate equation. Purified α4 and α4 mutant peptides (250 μg/ml) were incubated with increasing amounts of furin and PC5A, corresponding to an AMC release of 0.2–1.1 nmol/h. The extent of peptide cleavage was calculated by peak integration of RP-HPLC chromatograms and identification of the products was confirmed further by matrix-assisted laser-desorption ionization–time-of-flight MS (MALDI–TOF-MS) using a Voyageur DE-Pro instrument (PE-PerSeptive Biosystems) [30].

Metabolic radiolabelling

CHO-FD11/furin cells were co-transfected with 2 μg of the β1 recombinant vector and 6 μg of the pIRES2-EGFP vector alone or expressing WT α4, H592R or H592K using LIPOFECTAMINE™ 2000 reagent. The next day, cells were pulsed with 200 μCi/ml EasyTag Express [^{35}S]methionine/cysteine labelling mix (NEN Life Science, distributed by Mandel Scientific, Guelph, ON, Canada) for 1 h and chased for 2.5 h in DMEM with 10 % (v/v) FBS, supplemented with 240 mg/l cysteine and 150 mg/l methionine (both from Sigma), in the presence or absence of 15 mM NH_4Cl (Sigma). Cells were lysed in the presence of 10 mM EDTA and the lysates were analysed as described above.

Cell-adhesion assay

CHO-K1 cells were stably transfected with either empty pIRES2-EGFP vector or that expressing α4 or its R597A mutant (see above). Selected pools were checked for equivalent amount of surface α4 by FACS (see above) with a FACScalibur™ cytometer (BD Biosciences). Adhesion assays [32] were performed in 96-well plates coated overnight with 1 μg/ml human recombinant VCAM-1 (R&D Systems, Minneapolis, MN, U.S.A.) and blocked with BSA. Stable pools were resuspended with Versene (Invitrogen), rinsed twice with 1 % (v/v) BSA in RPMI 1640 medium to remove EDTA and 3×10^5 cells/well were incubated for 30 min at 37 °C in the same medium. Non-adherent cells were removed by four washes with 1 % (v/v) BSA in RPMI 1640 medium and adherent cells were quantified by monitoring the endogenous phosphatase activity [32].

RESULTS

Processing of α4 is blocked by α1-PDX

In order to verify whether or not PCs are involved in the processing of α4 integrin, we analysed its cleavage in Jurkat cells, a lymphoid-derived CD4$^+$ cell line which expresses furin, PC7 and PC5 [21]. The fate of α4 was followed by cell-surface biotinylation, immunoprecipitation of cell extracts with an anti-α4 mAb, SDS/PAGE (6 % gel) under non-reducing conditions, blotting and revelation with streptavidin–HRP. As seen in Figure 2, the endogenous 150 and 180 kDa pro-α4 is partially processed into N-terminal and C-terminal fragments of 80 and 70 kDa respectively [10], whereas no detectable processing occurred in the presence of α1-PDX. This result strongly suggests the implication of one or more PCs in pro-α4 maturation in Jurkat cells. Furthermore, flow cytometric analysis demonstrated that the cell-surface level of α4 was not affected by PC inhibition (results not shown).

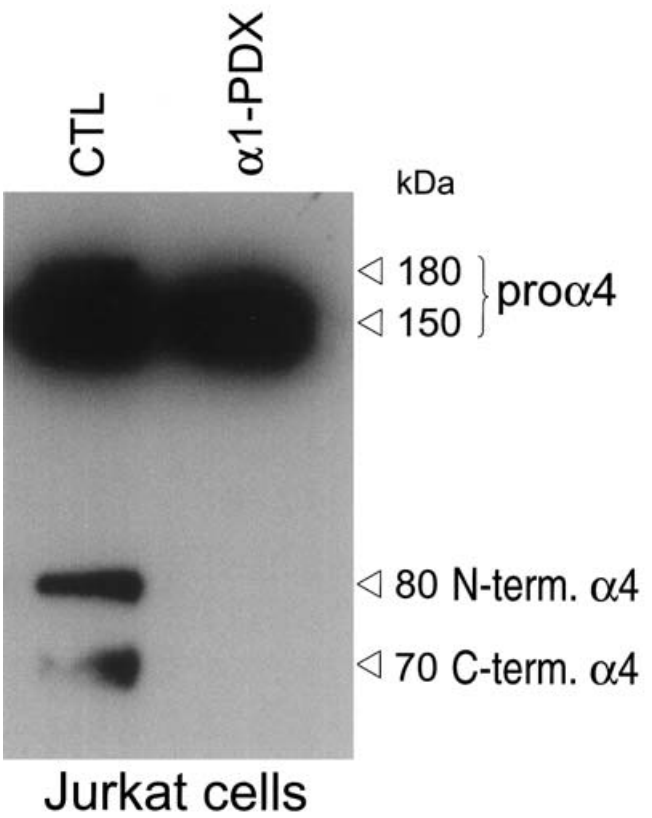

Figure 2 Inhibition of α4 processing by α1-PDX

Stably transfected Jurkat cells expressing the empty (CTL) or α1-PDX recombinant pcDNA3 vector were cell-surface biotinylated and lysed in the presence of SDS and EDTA. After α4 immunoprecipitation, SDS/PAGE (6 % gel) under non-reducing conditions and blotting, biotinylated proteins were revealed with streptavidin–HRP. Open arrowheads indicate the positions of pro-α4 and mature N- and C-terminal (term.) α4 fragments. A long exposure was shown to visualize the α4 products better.

Processing of α4 is performed best by furin and PC5A

To define which PC(s) can process α4, we chose to co-infect the furin-deficient LoVo cells [33], in which α4 is barely processed (WT; Figure 3), with recombinant VVs of α4 with each PC [21]. Co-expression of PC5A (the most effective), PACE4 or furin and, to a lesser extent, PC1 and PC5B resulted in a substantial increase in α4 maturation, while full-length or soluble (BTMD-) PC7 did not process this precursor. The soluble PC5A was more effective in processing pro-α4 than its membrane-bound isoform PC5B, as previously observed for other α integrins [15]. However, engineered soluble forms of furin and PC7 (BTMD) did not show an increased activity, suggesting that the lower efficiency of PC5B may rather result from the localization of PC5B in early compartments of the secretory pathway (brefeldin A-dispersible) [34].

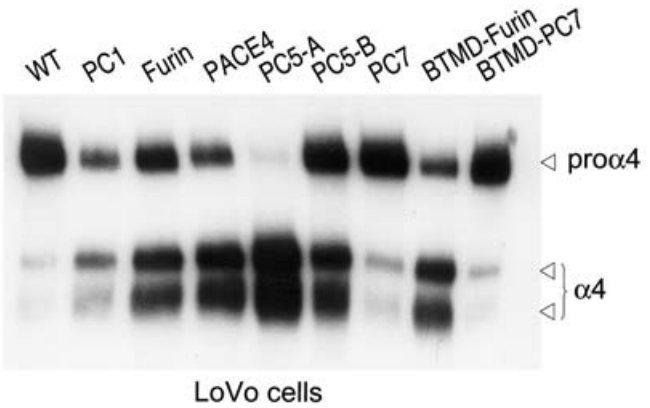

Figure 3 Cleavage of α4 by proproptein convertases

LoVo cells were co-infected with 1 plaque-forming unit (pfu) of α4 recombinant VV and 1 pfu of WT, PC1, furin, PACE4, PC5A, PC5B, PC7, BTMD-furin or BTMD-PC7 recombinant VV. After 16 h, cells were biotinylated, lysed and the α4-immunoprecipitated products were separated by non-reducing SDS/PAGE (6 % gel). Following blotting, immunoprecipitated proteins were revealed with streptavidin–HRP. Open arrowheads point to pro-α4 and mature α4 species.

We next evaluated the extent of the endogenous α4 maturation in six leucocyte-derived cell lines (Figure 4A) whose endogenous furin levels were estimated by Northern blot analyses (Figure 4B) and by RT-PCR for PC5, PACE4 and PC7. Although the efficiency of α4 processing (U937, 89 % > Jurkat, 52 % > HL60, 32 % ≈ SupT1, 31 % ≈ CEM, 28 % > CEM-T4, 22 %) generally correlates with the furin mRNA levels (Figure 4B), the presence of the other PCs, especially PC5, may contribute to the overall processing profile of each cell line. Both VV expression (Figure 3) and stable expression of PC7 in Jurkat cells (results not shown) clearly demonstrated that PC7 does not process pro-α4 integrin. The contribution of PACE4 also seems minor, since its presence in HL60 does not seem to significantly enhance processing as compared with all the other cell lines that do not express it. Thus it seems that furin and PC5 are the main cognate convertases of pro-α4. Indeed, the correlation of processing with furin mRNA levels was not perfect since furin mRNAs were approx. 2-fold more abundant in HL60 than in SupT1 cells for a similar extent of pro-α4 maturation. This could be explained either by a specific cell type environment or by the contribution of PC5 in pro-α4 processing.

Since furin and PC5 are expressed in many cell types containing α4 integrin and neither PACE4 or PC1 was detected in tested T4-lymphocyte cell lines [21], we focused on these two enzymes. Their processing activity was assayed in CEM-T4 cells in which endogenous α4 processing is low. We used the bicistronic vector pIRES2-EGFP to select for stable furin- or PC5A-transfected pools expressing similar levels of EGFP. As shown in Figure 5, furin (96 %) and PC5A (88 %) highly increase pro-α4 processing. We also observed some co-immunoprecipitation of β1 integrin, since, in this case, we omitted EDTA and SDS from the lysis buffer [8]. The fact that PC5A is almost as potent as furin in CEM-T4 stable transfections compared with LoVo cells VV infections may be related to the different expression systems used or to cell-type-specific properties. Expression of furin and PC5A could also increase α4 processing in Jurkat cells, whereas the membrane-bound PC5B and PC7 could not (results not shown), confirming the ability of these two PCs to cleave α4 in more than one $CD4^+$ cell line.

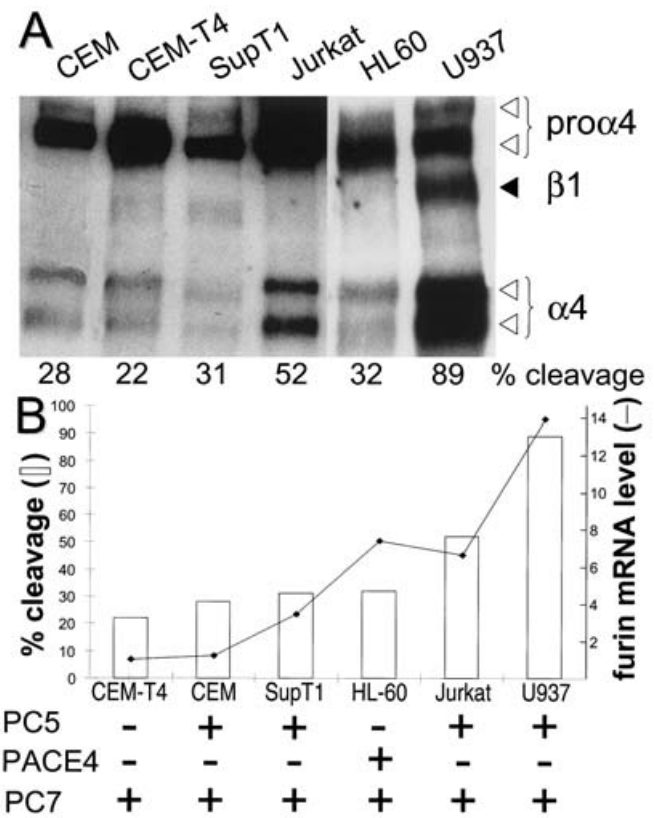

Figure 4 Correlation between the extent of pro-α4 processing and furin-expression level in human leucocytic cell lines

(**A**) Following cell-surface biotinylation and lysis, anti-α4-immunoprecipitated proteins were separated by SDS/PAGE (6 % gel) under non-reducing conditions, blotted and revealed with streptavidin–HRP. Open arrowheads indicate the positions of pro-α4 and α4 species, and the black arrowhead points to that of the co-immunoprecipitated β1 integrin (best visualized in U937 cells). The percentage processing values were calculated (see the Experimental section) by scanning of films exposed for various times. (**B**) Northern blot analysis of human furin and RT-PCR of PC5, PACE4 and PC7 in human leucocytic cell lines. Furin mRNA level were derived from phosphor screen scanning of ^{32}P-labelled cRNA hybridized membranes. Furin levels were normalized to the ribosomal 18 S RNA probe signal. The points illustrate relative furin mRNA levels (right-hand y-axis) and the histogram bars indicate the pro-α4 processing extent (left-hand y-axis). The line between furin expression level points was traced to visualize the correlation between the two parameters. The results of RT-PCR emphasize the endogenous presence (+) or absence (−) of PC5, PACE4 or PC7 mRNAs in these cells.

In vitro and e*x vivo* processing of α4 mutants

Since PCs often need a P6 arginine or lysine residue in the absence of a basic residue at P4 [35], we assessed the importance of the histidine residue at P6 (Figure 1) in α4 processing. Furin and PC5A were thus incubated with a high concentration (approx. 130 μM) of peptides mimicking the WT site (LGP**H**V-IS**KR**^{597} ↓ STEEFPLQ) or its P6 mutants H592R and H592A and the percentage cleavage was monitored by RP-HPLC. WT and H592R peptides were similarly cut by either enzyme at pH 7.0 (Figure 6). In contrast, the H592A peptide is not cleaved at all by furin and only approx. 2-fold less efficiently by PC5A. These results suggest a more stringent requirement for a P6 positively charged residue for furin than for PC5A.

To test the hypothesis that a positive charge at P6 may regulate processing, we transiently expressed α4 integrin mutants (P6, H592R, H592K, H592E, H592A and H592L; P1, R597A) in CHO-K1 cells and analysed their cleavage (Figure 7). Similar signal intensities suggest that the α4 mutants were expressed and reached the cell surface as well as WT α4. The R597A mutation

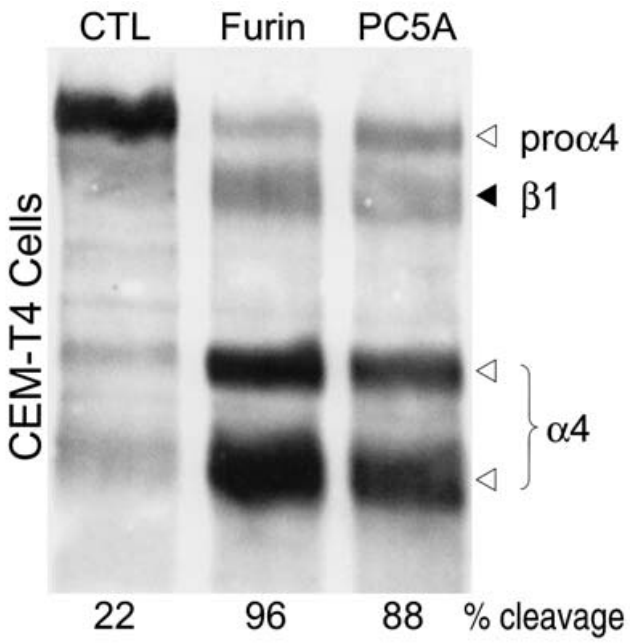

Figure 5 Stable expression of furin and PC5A increases pro-α4 endoproteolysis in the CD4$^+$ lymphocyte cell line CEM-T4

CEM-T4 cells were stably transfected with empty vector (CTL), furin or PC5A. The pools of cell-surface proteins were biotinylated, lysed and immunoprecipitated with an α4 mAb. Immunoprecipitated proteins were separated by SDS/PAGE (6% gel) under non-reducing conditions, followed by revelation with streptavidin–HRP. The migration positions of pro-α4, α4 fragments (open arrowheads) as well as the co-immunoprecipitated β1 integrin (closed arrowhead) are shown. Calculation of the percentage processing was acheived with the densitometric data acquired from STORM imaging (see the Experimental section).

was the only one that abrogated α4 processing, and the H592E, H592A and H592L mutations reduced pro-α4 processing by 39, 71 and 66% respectively. Unexpectedly, the glutamate substitution seemed to be preferred to alanine and leucine. Whereas the mutant H592K maintained the α4-processing rate, the H592R mutation increased it. Thus, in contrast with *in vitro* experiments in which the H592R peptide was as well cleaved as the WT one, *ex vivo*, the H592R mutation led to a 25% increase in pro-α4 processing (Figure 7).

In vitro analysis of the pH-dependent processing of WT α4 and its H592R mutant

To correlate the extent of positive charge of the P6 histidine residue and the pH dependence of the processing efficacy of pro-α4 by furin and PC5A, we synthesized two intramolecular QFPs, α4-QFP and α4-QFP-H592R, encompassing the α4 cleavage site, Abz-GP**H**VISKR^{597}↓STE-Tyx-A and its H592R mutant. Its cleavage at Arg^{597} was confirmed by RP-HPLC and MALDI–TOF-MS identification of the products [30] (results not shown). Digestion was performed using a fixed activity of either furin or PC5A, releasing 0.5 nmol of AMC from the substrate pERTKR-MCA in 1 h at pH 7.4, and increasing amounts of α4-QFP or α4-QFP-H592R. The released Abz-GPHVISKR^{597} product at both pH 6.0 and 7.4 was measured by fluorimetry [30] and the apparent V_{max} and K_m were determined using Michaelis–Menten plots. The pH-dependence of the V_{max}/K_m is depicted in Figure 8. Whereas PC5A cleaves the H592R substrate approx. 3-fold more effectively at pH 7.4 compared with that at pH 6.0, furin is similarly active at both pHs. This reveals that on favourable substrates that do not

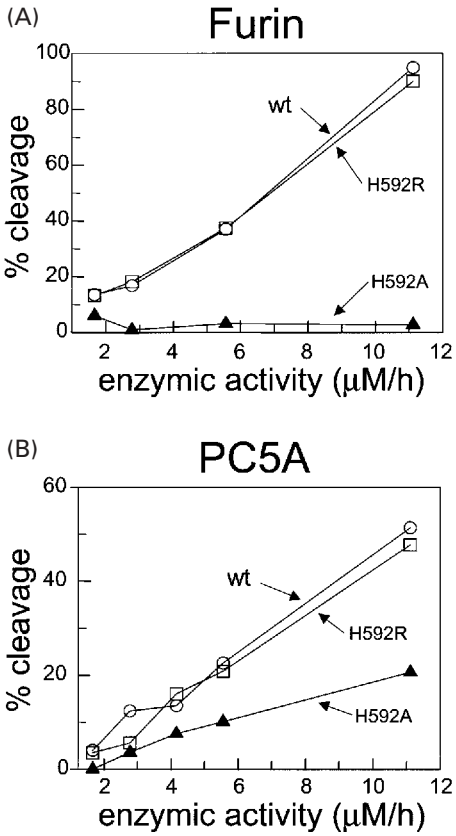

Figure 6 *In vitro* processing of WT and mutant peptides encompassing the α4 processing site

Identical concentrations of 17-mer (approx. 130 μM) α4 and mutant peptides were incubated with increasing amounts of furin (**A**) or PC5A (**B**) activity (pERTKR-MCA fluorogenic PC substrate) for 15 min at room temperature in 100 μl Tris (20 mM, adjusted with ethanoic acid to pH 7.0) with 2 mM calcium chloride. Product appearance was measured by RP-HPLC by integration of the products and initial peptide peaks. α4wt (○), H592R (□) and H592A (▲).

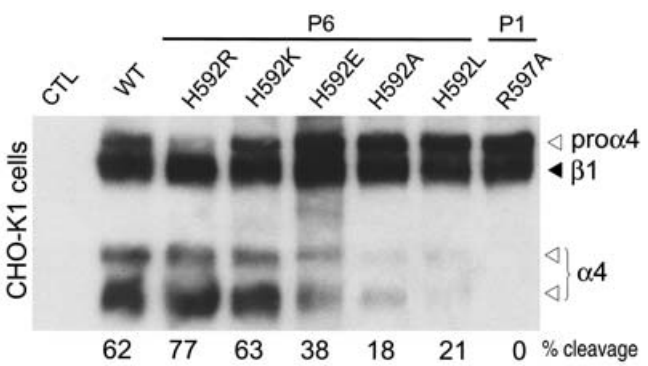

Figure 7 Cellular processing of pro-α4 cleavage-site mutants

CHO-K1 cells were transfected with WT α4, H592R, H592K, H592E, H592A and H592L recombinant vectors. Cell-surface proteins were biotinylated, lysed and immunoprecipitated with an α4 mAb. Immunoprecipitated proteins were separated by SDS/PAGE (6% gel) under non-reducing conditions, followed by the revelation with streptavidin–HRP. The migration positions of pro-α4, α4 fragments (open arrowheads) as well as the co-immunoprecipitated β1 integrin (closed arrowhead) are indicated. Percentage processing was calculated with the densitometric data acquired from STORM™ imaging (see the Experimental section).

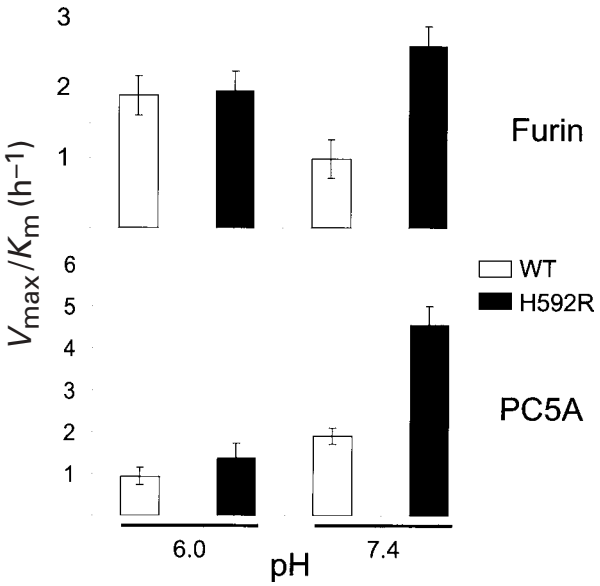

Figure 8 pH-dependence of the *in vitro* processing of WT and H592R quenched α4-fluorogenic substrates

Apparent V_{max} and K_m values were determined by the digestion by either furin or PC5A of increasing concentrations (0.3–25.7 μM) of the internally QFPs, α4-QFP and α4-QFP-H592R at pH 6.0 and 7.4. The released Abz-GPHVISKR^{597} product was measured by fluorimetry and derived initial rates were fitted to the Michaelis–Menten equation. Results are the mean ratios of V_{max} to K_m $\pm$ S.E.M.

contain histidine, the activity of both convertases is optimal at neutral pH, a condition best favouring PC5A activity. In contrast, the WT peptide is cleaved best by furin at pH 6.0 and by PC5A at pH 7.4 (Figure 8). We surmise that, since in the WT peptide histidine occupies the P6 position, its pH-dependent charge neutralization may negatively regulate the extent of α4 processing, such that when the histidine residue is positively charged (pH 6.0), α4 may be optimally cleaved by furin, but not by PC5A.

The P6 histidine limits α4 processing to acidic secretory compartments

The above *in vitro* results demonstrate the necessity of a positively charged P6 residue for α4 endoproteolysis by furin (Figures 5 and 8). Previous studies [31,35] demonstrated that, in the absence of a P4 basic residue, furin activity is enhanced by a P2 or P6 basic residue, suggesting that the P6 histidine contribution to α4 processing could vary depending on its protonation state. Since the charge on histidine side chains (pK_a approx. 6.5) is highly susceptible to a physiological shift of pH present along the secretory pathway [36], we hypothesized that the P6 histidine becomes more positively charged as α4 traffics to the *trans*-Golgi network (TGN) (pH approx. 5.9–6.3) and less so upon reaching the cell surface. This suggested that pro-α4 processing by furin could be pH-dependent. To verify this hypothesis, and since furin concentrates in the TGN, we examined the effect of 15 mM NH_4Cl that should neutralize the pH of the TGN from approx. 5.9 to approx. 6.8 [37]. Since furin-deficient CHO cells (FD11) do not process pro-α4 (pulse–chase experiment; results not shown), and to specifically assess the extent of NH_4Cl inhibition of the furin-processing of pro-α4, we decided to transfect CHO-FD11 stably expressing furin [26]. As controls, we also analysed the H592R and H592K mutants (pK_a of arginine and lysine side chains approx. 12.5 and 10.5 respectively) whose processing is expected not to be significantly inhibited by NH_4Cl. Short incubations and

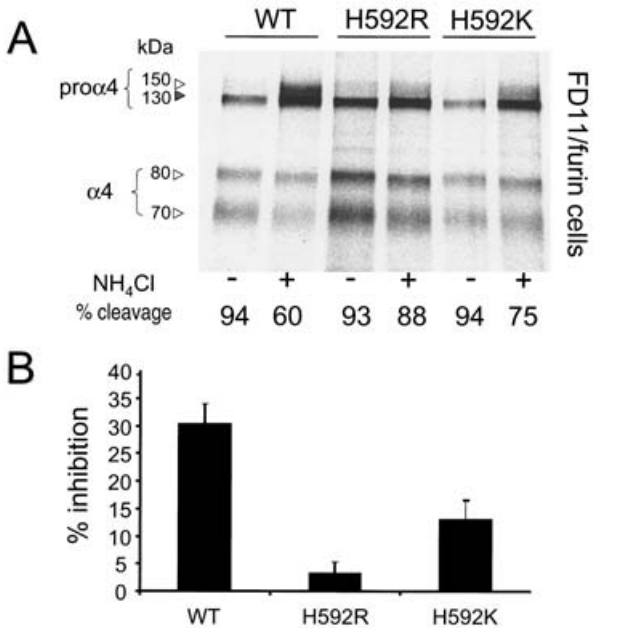

Figure 9 NH_4Cl inhibition of furin-generated pro-α4 processing

(**A**) CHO-FD11/furin cells were transfected with WT α4, H592R and H592K recombinant vectors. Cells were pulse-labelled for 60 min and chased for 150 min in the absence ($-$) or presence ($+$) of NH_4Cl. Cells were lysed in the presence of EDTA and were immunoprecipitated with an α4 mAb. Immunoprecipitated proteins were separated by SDS/PAGE (6 % gel) under non-reducing conditions and quantified (see the Experimental section). EndoH-resistant (150 kDa; open arrowheads) and endoH-sensitive (130 kDa; closed arrowhead) α4 forms are indicated. The slightly faster migration of the 150 kDa and 80 kDa products observed in the presence of NH_4Cl may be due to reduced sialylation [50]. (**B**) Quantification of the percentage processing inhibition in the presence of NH_4Cl compared with that of the untreated cells using the percentage cleavage data in (**A**) derived from STORM^{TM} quantification.

relatively low concentrations (15 mM) of NH_4Cl were selected to minimize undesired effects, such as inhibition of furin activation [18] and/or modulation of its trafficking [38].

Transfected CHO-FD11/furin cells were pulse-labelled for 1 h and chased for 150 min in the presence or absence of 15 mM NH_4Cl (Figure 9). To facilitate α4 analysis, immunoprecipitation of cell lysates was performed in the presence of EDTA to disrupt the $\alpha4\beta1$ dimers. The 130 kDa pro-α4 corresponds to endoglycosidase-H (endoH)-sensitive species still present in the ER (and hence are not cleavable by furin), and the 150 kDa endoH-resistant form of pro-α4 is the precursor form that is processed [9]. The percentage of pro-α4 processing was thus calculated as the ratio of the normalized 80 kDa product [21 cysteine + methionine] over that of the total normalized endoH-resistant [80 kDa (21 cysteine + methionine) + 150 kDa (44 cysteine + methionine)] species. In stable pools of CHO-FD11/furin, and in the absence of NH_4Cl, WT pro-α4 and its mutants were equally processed (approx. 93–94 %, Figure 9). In the presence of NH_4Cl, processing of WT pro-α4 was inhibited by 36 % (decrease in percentage cleavage from 94 % to 60 %), while that of the H592K and H592R mutants was minimally inhibited (20 % and 5 % respectively; Figure 9). This suggests that the P6 histidine enhances the sensitivity of pro-α4 processing to pH modulation by NH_4Cl.

Cleavage of α4 does not modify adhesion *in vitro*

It was shown that overexpression in K562 cells of a non-cleavable R597L α4 mutant did not affect $\alpha4\beta1$ adhesion on fibronectin

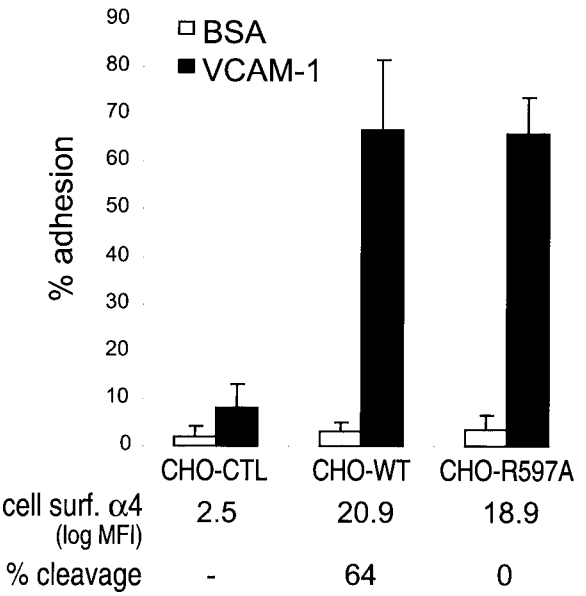

Figure 10 Adhesion of α4 transfectants to VCAM-1

Cells were incubated in 96-well coated plates with BSA (open bars) or VCAM-1 (closed bars; 1 μg/ml). After 30 min adhesion, non-adherent cells were washed away and bound cell fractions (in triplicate) were counted by monitoring the endogenous phosphatase activity [32]. α4 cell surface (cell surf. α4) expression was measured by flow cytometry and the surface cleavage extent was calculated as described in the Experimental section.

or VCAM-1 [8]. To verify whether or not the extent of pro-α4 cleavage modulates adhesion to VCAM-1 in CHO-K1 cells, we produced stable transfectants expressing the empty vector (CHO-CTL), WT α4 (CHO-WT) or its uncleavable R597A variant (CHO-R597A). Stably transfected cells twice underwent FACS to select pools that express equivalent amounts of surface α4. As expected, no cleavage was observed for the R597A mutant, whereas the rate of cleavage observed for WT (64 %; Figure 10) was similar to that obtained in transient transfected cells (62 %; Figure 7). Finally, the generated cell pools were incubated on immobilized VCAM-1, an α4 ligand, for 30 min at 37 °C. The bound cell fraction was quantified by densitometry. The α4 specificity of the binding was demonstrated by the absence of binding to BSA and low adhesion of CHO-CTL cells to VCAM-1 (Figure 10). However, under these conditions, α4 and its uncleavable pro-α4 form shared the same adhesion properties. We thus conclude that pro-α4 cleavage does not affect the adhesion of either CHO cells (the present study) or K562 cells [8] to VCAM-1.

DISCUSSION

In the present study, we investigated the processing of the human integrin α4 subunit. Our results demonstrate that the cleavage of pro-α4 (150 kDa) at the HVISKR^{597} ↓ ST sequence in Jurkat cells was completely inhibited by the PC inhibitor α1-PDX (Figure 2) and the R597A mutation (Figure 7). Co-expression in LoVo-C5 cells of α4 and PCs revealed that furin and PC5A efficiently processed pro-α4 (Figure 3), suggesting their implication in this maturation event. The extent of the α4 endogenous cleavage in five haematopoietic cell lines (22–89 %) generally correlated with their furin and PC5 mRNA expression (Figure 4). In the CEM-T4 cell line, which has the lowest levels of pro-α4 processing and furin and PC5 mRNAs, stable expression of furin and PC5A increased the α4 maturation level from 22 % to 96 % and 88 % respectively (Figure 5).

PC5A-recombinant VV infection of LoVo cells led to a better rate of pro-α4 processing than furin-recombinant VV infection (Figure 3) and, *in vitro*, both enzymes cleaved the QFP-α4 peptide encompassing the α4 processing site (see below). Thus our overall results are in favour of a predominant role of furin and/or PC5 in α4 processing in a cell-type-dependent fashion. This conclusion is reinforced by the following findings: (i) extremely low pro-α4 cleavage levels in two furin-deficient cell lines, LoVo (Figure 3) and CHO-FD11, both of which express very low levels of PC5 (results not shown); (ii) 100 % processing of exogenous pro-α4 in the highest furin-expressing cell line K562 ([8], and results not shown), whereas it was 89 % cleaved in U937 cells expressing about 2-fold less furin mRNA; and (iii) following lymphocyte activation, the increase in pro-α4 processing [10] correlates with the up-regulation of the mRNA levels of furin, but not with the invariant PC5 mRNA transcripts [29].

Generally, effective furin processing of precursors requires the presence of a P1 arginine residue and at least one, or better still two, additional arginine or lysine residues at P2 and P4, P2 and P6, or P4 and P6 positions [31,35,39]. The absence of a P4 or P6 arginine or lysine residue, but the presence of a P6 histidine residue are distinguishing features of group II α integrins (Figure 1), as compared with the majority of known furin substrates [14]. We thus examined the role of the P6 histidine and its variants in pro-α4 processing by either *in vitro* digestions of peptides mimicking the pro-α4 cleavage site (Figures 6 and 8) or *ex vivo* processing of WT and mutant forms of pro-α4 (Figure 7).

In vitro, at high peptide concentrations (approx. 130 μM), although alanine substitution for the P6 histidine completely abolished furin cleavage and significantly reduced PC5A processing (Figure 6), arginine substitution did not significantly affect the peptide cleavage by either enzyme at pH 7.0. Thus, under optimal substrate concentrations, furin does not cleave α4 peptides that lack a positively charged amino acid at the P6 position. Kinetic analysis using limiting concentrations of QFPs showed that, at pH 7.4, both furin and PC5A prefer the H592R substrate (Figure 8). In contrast, the WT peptide is cleaved best by furin at pH 6.0. We have thus demonstrated for the first time that a histidine residue at P6 and its protonation state may be as crucial as arginine in furin-recognition motifs in which there is no basic amino acid at P4. PC5 was less stringent in its requirement for upstream basic residues, an observation supported by a recent *in vitro* PC5 study [40], and seems to prefer cleavage at neutral pHs, as previously reported for other substrates [15,21,35]. The impact of different P6 substitutions on pro-α4 processing was also assessed *ex vivo* (Figure 7). In agreement with the kinetics of the *in vitro* study at pH 7.4 using QFPs (Figure 8), arginine at P6 enhanced processing, indicating that the endogenous pro-α4 cleavage in CHO-K1 cells is dependent on the presence of a positively charged residue at P6, and possibly occurs at pHs closer to neutrality. Furthermore, while P6 alanine and leucine substitutions did not completely block α4 cleavage, the P1 alanine substitution for arginine abolished it. Similarly, Teixido et al. [8] observed either a partial (P2 Lys → Gln) or total (P1 Arg → Leu) blockade of pro-α4 processing with their mutants. This suggests that, although P1 is the most critical position, the P2 and P6 positions are not essential for cleavage, but greatly enhance the extent of processing.

In the present study, we examined the impact of the P6 histidine residue on the pH sensitivity of pro-α4 cleavage by PC5A and/or furin both *in vitro* (Figure 8) and *ex vivo* (Figure 9). The

in vitro results clearly show that furin best cleaves the WT peptide at acidic pH, whereas the reverse is true for PC5A (Figure 8). In agreement, we showed that treatment of CHO-FD11 cells overexpressing furin with a low dose of 15 mM NH_4Cl, which increases the pH of organelles, led to a significant inhibition of WT pro-α4 maturation, whereas the lysine and, especially, the arginine P6 mutants were much less affected (Figure 9). The fact that the lysine mutant is also somewhat affected suggests that, aside from the P6 histidine effect, pH could also affect the overall conformation of the heterodimeric integrin and possibly furin activity. Notice that, in the present work, we have used 15 mM NH_4Cl rather than the 50 mM used for the furin work [38]. The high concentration of this agent may indeed affect endocytosis and/or furin trafficking. However, at the classical low dose < 20 mM, the effects on furin activation and/or recycling, and endocytosis are not known. Nevertheless, the observed differential effect of NH_4Cl was consistent in three separate experiments and the processing of the WT form was always the most affected one. Furin is mainly found in the TGN, but also transits to the cell surface where it is endocytosed and recycled back to the TGN [14]. At the cell surface, furin processes the anthrax-toxin-protective antigen [14], thereby stimulating endocytosis of the toxin [41]. Furin was also reported to cleave a mutant insulin receptor in the neutral ER [42] and *Pseudomonas* exotoxin A within the acidic endosomes [14]. This suggests that furin is active not only in the TGN, but also in more (early endosomes) or less (cell surface, ER) acidic environments. We thus propose that the presence of a P6 histidine in furin substrates restricts their cleavage to acidic compartments of the secretory pathway, where histidine would be fully charged. In agreement, no cell-surface pro-α4 processing could be detected [9]. It is not yet known if histidine may replace a basic residue in P2 or P4. However, a natural P2 Arg $\rightarrow$ His mutation blocks proalbumin cleavage [43]. This study could be extended to substrates that, like α4, harbour a conserved P6 histidine residue in the presence of a P1 arginine residue and either a P2 or P4 arginine or lysine residue, including other members of group II α integrins (Figure 1), VEGF-C [44] and BMP-4 [45].

Finally, the *in vitro* adhesion properties to VCAM-1 of an uncleavable form of pro-α4 were similar to that of α4 (Figure 10), opening the question of the physiological function of pro-α4 processing. It was reported that processing pro-α6 is important for inside-out signalling [19]. However, our preliminary data with PMA activation of α4-CHO transfectants did not reveal a significant difference in adhesion on VCAM-1 between processed WT α4 and unprocessed R597A pro-α4 (results not shown). It may thus be necessary to find an *in vivo* model in order to gauge the importance of this processing, e.g. in knock-in transgenic mice expressing the R597A mutant. Of note, knockout studies in mice revealed that during embryogenesis, the $\alpha4\beta1$ integrin [46] and furin [47] are both required for chorioallantoic fusion and early cardiac development, suggesting that furin may be needed to process pro-α4 during development. Processing may also be important for the differential migration of activated lymphocytes to inflamed peripheral tissues such as in the central nervous system [48].

In conclusion, the past [15,16] and present data support the notion that furin and PC5A are the major candidate converting enzymes of all processed integrin α chains. Inhibition/silencing of one or both of these two convertases will probably lead to the complete abrogation of all pro-α chain processing. Our results further point out the importance of the P6 histidine in favouring an acidic milieu for the pro-α4 processing event to take place, a conclusion that may be extended to other precursors presenting a histidine at the vicinity of a PC-processing site. Indeed, most PCs exhibit a histidine residue at the P7 position of their secondary prosegment processing site [49], whose autocatalytic cleavage requires acidic pH and leads to enzyme activation [18]. Finally, P5 or P7 to P9 histidine residues may be responsible for the processing in endosomes, and not at the cell surface, of *Pseudomonas* exotoxin A at the R**H**RQPR$\downarrow$ site and Shiga SLT-1 toxin at the **HHH**ASRVAR$\downarrow$ sequence [14]. Our conclusions on the importance of histidine in regulating the processing of specific PC-substrates may thus extend to residues other than P6.

We acknowledge our appreciation to Dr A. Prat for her tremendous help in the writing of this manuscript. We also thank E. Marcinkiewicz, J. Hamelin, D. Gauthier, A. Lemieux, M.-C. Asselin and S. Benjannet for their technical help throughout this study. This work was supported by grants from the Medical Research Council of Canada, Group Grant GP-11474 and MGP-44363. We thank the CIHR for the salary support of E. B. (CIHR fellowship MST-34571). We also express our gratitude to N. Nour, B. B. Touré, Dr C. Lazure, Dr A. M. Khatib and Dr J. Cromlish for helpful discussions and advice, and to Dr A. Israël for the gift of Jurkat-α1-PDX cells. The secretarial assistance of Mrs Brigitte Mary is greatly appreciated.

REFERENCES

1 Lobb, R. R. and Hemler, M. E. (1994) The pathophysiologic role of α4 integrins *in vivo*. J. Clin. Invest. **94**, 1722–1728
2 Hynes, R. O. (2002) Integrins: bidirectional, allosteric signaling machines. Cell **110**, 673–687
3 Hemler, M. E., Elices, M. J., Parker, C. and Takada, Y. (1990) Structure of the integrin VLA-4 and its cell–cell and cell–matrix adhesion functions. Immunol. Rev. **114**, 45–65
4 Sengbusch, J. K., He, W., Pinco, K. A. and Yang, J. T. (2002) Dual functions of $\alpha4\beta1$ integrin in epicardial development: initial migration and long-term attachment. J. Cell Biol. **157**, 873–882
5 Berlin, C., Berg, E. L., Briskin, M. J., Andrew, D. P., Kilshaw, P. J., Holzmann, B., Weissman, I. L., Hamann, A. and Butcher, E. C. (1993) $\alpha4\beta7$ integrin mediates lymphocyte binding to the mucosal vascular addressin MAdCAM-1. Cell **74**, 185–185
6 Laschinger, M. and Engelhardt, B. (2000) Interaction of α4-integrin with VCAM-1 is involved in adhesion of encephalitogenic T cell blasts to brain endothelium but not in their transendothelial migration *in vitro*. J. Neuroimmunol. **102**, 32–43
7 Wayner, E. A., Garcia-Pardo, A., Humphries, M. J., McDonald, J. A. and Carter, W. G. (1989) Identification and characterization of the T lymphocyte adhesion receptor for an alternative cell attachment domain (CS-1) in plasma fibronectin. J. Cell Biol. **109**, 1321–1330
8 Teixido, J., Parker, C. M., Kassner, P. D. and Hemler, M. E. (1992) Functional and structural analysis of VLA-4 integrin α4 subunit cleavage. J. Biol. Chem. **267**, 1786–1791
9 Bednarczyk, J. L., Szabo, M. C. and McIntyre, B. W. (1992) Post-translational processing of the leukocyte integrin $\alpha4\beta1$. J. Biol. Chem. **267**, 25274–25281
10 Blue, M. L., Davis, G., Conrad, P. and Kelley, K. (1993) Specific cleavage of the α4 integrin associated with activation of peripheral T lymphocytes. Immunology **78**, 80–85
11 Xiong, J. P., Stehle, T., Zhang, R., Joachimiak, A., Frech, M., Goodman, S. L. and Arnaout, M. A. (2002) Crystal structure of the extracellular segment of integrin $\alpha V\beta3$ in complex with an Arg-Gly-Asp ligand. Science **296**, 151–155
12 Dedhar, S. (1999) Integrins and signal transduction. Curr. Opin. Hematol. **6**, 37–43
13 Seidah, N. G. and Chretien, M. (1999) Proprotein and prohormone convertases: a family of subtilases generating diverse bioactive polypeptides. Brain Res. **848**, 45–62
14 Thomas, G. (2002) Furin at the cutting edge: from protein traffic to embryogenesis and disease. Nat. Rev. Mol. Cell Biol. **3**, 753–766
15 Lissitzky, J. C., Luis, J., Munzer, J. S., Benjannet, S., Parat, F., Chretien, M., Marvaldi, J. and Seidah, N. G. (2000) Endoproteolytic processing of integrin pro-α subunits involves the redundant function of furin and proprotein convertase (PC) 5A, but not paired basic amino acid converting enzyme (PACE) 4, PC5B or PC7. Biochem. J. **346**, 133–138
16 Lehmann, M., Rigot, V., Seidah, N. G., Marvaldi, J. and Lissitzky, J. C. (1996) Lack of integrin α-chain endoproteolytic cleavage in furin-deficient human colon adenocarcinoma cells LoVo. Biochem. J. **317**, 803–809
17 Rigot, V., Andre, F., Lehmann, M., Lissitzky, J. C., Marvaldi, J. and Luis, J. (1999) Biogenesis of $\alpha6\beta4$ integrin in a human colonic adenocarcinoma cell line involvement of calnexin. Eur. J. Biochem. **261**, 659–666
18 Anderson, E. D., VanSlyke, J. K., Thulin, C. D., Jean, F. and Thomas, G. (1997) Activation of the furin endoprotease is a multiple-step process: requirements for acidification and internal propeptide cleavage. EMBO J. **16**, 1508–1518

19 Delwel, G. O., Kuikman, I., van der Schors, R. C., de Melker, A. A. and Sonnenberg, A. (1997) Identification of the cleavage sites in the α6A integrin subunit: structural requirements for cleavage and functional analysis of the uncleaved α6Aβ1 integrin. Biochem. J. **324**, 263–272
20 Anderson, E. D., Thomas, L., Hayflick, J. S. and Thomas, G. (1993) Inhibition of HIV-1 gp160-dependent membrane fusion by a furin-directed α1-antitrypsin variant. J. Biol. Chem. **268**, 24887–24891
21 Decroly, E., Wouters, S., Di Bello, C., Lazure, C., Ruysschaert, J. M. and Seidah, N. G. (1996) Identification of the paired basic convertases implicated in HIV gp160 processing based on *in vitro* assays and expression in $CD4^+$ cell lines. J. Biol. Chem. **271**, 30442–30450
22 Benjannet, S., Savaria, D., Laslop, A., Munzer, J. S., Chretien, M., Marcinkiewicz, M. and Seidah, N. G. (1997) α1-antitrypsin Portland inhibits processing of precursors mediated by proprotein convertases primarily within the constitutive secretory pathway. J. Biol. Chem. **272**, 26210–26218
23 Berthet, V., Rigot, V., Champion, S., Secchi, J., Fouchier, F., Marvaldi, J. and Luis, J. (2000) Role of endoproteolytic processing in the adhesive and signaling functions of αvβ5 integrin. J. Biol. Chem. **275**, 33308–33313
24 Khatib, A. M., Siegfried, G., Chretien, M., Metrakos, P. and Seidah, N. G. (2002) Proprotein convertases in tumor progression and malignancy: novel targets in cancer therapy. Am. J. Pathol. **160**, 1921–1935
25 Zamir, E. and Geiger, B. (2001) Molecular complexity and dynamics of cell–matrix adhesions. J. Cell Sci. **114**, 3583–3590
26 Gordon, V. M., Klimpel, K. R., Arora, N., Henderson, M. A. and Leppla, S. H. (1995) Proteolytic activation of bacterial toxins by eukaryotic cells is performed by furin and by additional cellular proteases. Infect. Immun. **63**, 82–87
27 Logeat, F., Bessia, C., Brou, C., LeBail, O., Jarriault, S., Seidah, N. G. and Israel, A. (1998) The Notch1 receptor is cleaved constitutively by a furin-like convertase. Proc. Natl. Acad. Sci. U.S.A. **95**, 8108–8112
28 Seidah, N. G., Chretien, M. and Day, R. (1994) The family of subtilisin/kexin like pro-protein and pro-hormone convertases: divergent or shared functions. Biochimie **76**, 197–209
29 Decroly, E., Benjannet, S., Savaria, D. and Seidah, N. G. (1997) Comparative functional role of PC7 and furin in the processing of the HIV envelope glycoprotein gp160. FEBS Lett. **405**, 68–72
30 Basak, A., Zhong, M., Munzer, J. S., Chretien, M. and Seidah, N. G. (2001) Implication of the proprotein convertases furin, PC5 and PC7 in the cleavage of surface glycoproteins of Hong Kong, Ebola and respiratory syncytial viruses: a comparative analysis with fluorogenic peptides. Biochem. J. **353**, 537–545
31 Lazure, C., Gauthier, D., Jean, F., Boudreault, A., Seidah, N. G., Bennett, H. P. and Hendy, G. N. (1998) *In vitro* cleavage of internally quenched fluorogenic human proparathyroid hormone and proparathyroid-related peptide substrates by furin. Generation of a potent inhibitor. J. Biol. Chem. **273**, 8572–8580
32 Akatsu, T., Ono, K., Murakami, T., Katayama, Y., Nishikawa, M., Wada, S., Yamamoto, M., Kugai, N., Matsuura, N., Takada, Y. and Nagata, N. (1998) Chinese hamster ovary cells expressing α4β1 integrin stimulate osteoclast formation *in vivo*. J. Bone Miner. Res. **13**, 1251–1259
33 Takahashi, S., Kasai, K., Hatsuzawa, K., Kitamura, N., Misumi, Y., Ikehara, Y., Murakami, K. and Nakayama, K. (1993) A mutation of furin causes the lack of precursor-processing activity in human colon carcinoma LoVo cells. Biochem. Biophys. Res. Commun. **195**, 1019–1026
34 Xiang, Y., Molloy, S. S., Thomas, L. and Thomas, G. (2000) The PC6B cytoplasmic domain contains two acidic clusters that direct sorting to distinct *trans*-Golgi network/endosomal compartments. Mol. Biol. Cell **11**, 1257–1273
35 Krysan, D. J., Rockwell, N. C. and Fuller, R. S. (1999) Quantitative characterization of furin specificity. Energetics of substrate discrimination using an internally consistent set of hexapeptidyl methylcoumarinamides. J. Biol. Chem. **274**, 23229–23234
36 Wu, M. M., Grabe, M., Adams, S., Tsien, R. Y., Moore, H. P. and Machen, T. E. (2001) Mechanisms of pH regulation in the regulated secretory pathway. J. Biol. Chem. **276**, 33027–33035
37 Demaurex, N., Furuya, W., D'Souza, S., Bonifacino, J. S. and Grinstein, S. (1998) Mechanism of acidification of the *trans*-Golgi network (TGN). *In situ* measurements of pH using retrieval of TGN38 and furin from the cell surface. J. Biol. Chem. **273**, 2044–2051
38 Chapman, R. E. and Munro, S. (1994) Retrieval of TGN proteins from the cell surface requires endosomal acidification. EMBO J. **13**, 2305–2312
39 Watanabe, T., Murakami, K. and Nakayama, K. (1993) Positional and additive effects of basic amino acids on processing of precursor proteins within the constitutive secretory pathway. FEBS Lett. **320**, 215–218
40 Cain, B. M., Vishnuvardhan, D., Wang, W., Foulon, T., Cadel, S., Cohen, P. and Beinfeld, M. C. (2002) Production, purification, and characterization of recombinant prohormone convertase 5 from baculovirus-infected insect cells. Protein Expression Purif. **24**, 227–233
41 Beauregard, K. E., Collier, R. J. and Swanson, J. A. (2000) Proteolytic activation of receptor-bound anthrax protective antigen on macrophages promotes its internalization. Cell. Microbiol. **2**, 251–258
42 Bass, J., Turck, C., Rouard, M. and Steiner, D. F. (2000) Furin-mediated processing in the early secretory pathway: sequential cleavage and degradation of misfolded insulin receptors. Proc. Natl. Acad. Sci. U.S.A. **97**, 11905–11909
43 Brennan, S. O. and Nakayama, K. (1994) Cleavage of proalbumin peptides by furin reveals unexpected restrictions at the P2 and P'1 sites. FEBS Lett. **347**, 80–84
44 Nour, N., Basak, A., Chretien, M. and Seidah, N. G. (2003) Structure–function analysis of the proprotein convertase PC5A. J. Biol. Chem. **278**, 2886–2895
45 Cui, Y., Hackenmiller, R., Berg, L., Jean, F., Nakayama, T., Thomas, G. and Christian, J. L. (2001) The activity and signaling range of mature BMP-4 is regulated by sequential cleavage at two sites within the prodomain of the precursor. Genes Dev. **15**, 2797–2802
46 Yang, J. T., Rayburn, H. and Hynes, R. O. (1995) Cell adhesion events mediated by α4 integrins are essential in placental and cardiac development. Development **121**, 549–560
47 Roebroek, A. J., Umans, L., Pauli, I. G., Robertson, E. J., van Leuven, F., Van de Ven, W. J. and Constam, D. B. (1998) Failure of ventral closure and axial rotation in embryos lacking the proprotein convertase Furin. Development **125**, 4863–4876
48 Graesser, D., Mahooti, S., Haas, T., Davis, S., Clark, R. B. and Madri, J. A. (1998) The interrelationship of α4 integrin and matrix metalloproteinase-2 in the pathogenesis of experimental autoimmune encephalomyelitis. Lab. Invest. **78**, 1445–1458
49 Seidah, N. G., Day, R., Marcinkiewicz, M. and Chretien, M. (1998) Precursor convertases: an evolutionary ancient, cell-specific, combinatorial mechanism yielding diverse bioactive peptides and proteins. Ann. N. Y. Acad. Sci. **839**, 9–24
50 Zanghi, J. A., Mendoza, T. P., Knop, R. H. and Miller, W. M. (1998) Ammonia inhibits neural cell adhesion molecule polysialylation in Chinese hamster ovary and small cell lung cancer cells. J. Cell Physiol. **177**, 248–263

Received 18 October 2002/17 March 2003; accepted 14 April 2003
Published as BJ Immediate Publication 14 April 2003, DOI 10.1042/BJ20021630